

STRUCTURE AND PROPERTIES OF THE DEFORMED STATE

Effect of the Deformation Axis Orientation on the Strength of Dislocation Junctions in FCC Single Crystals

R. I. Kurinnaya^{a, *}, M. V. Zgolich^a, V. A. Starenchenko^a, M. V. Matveev^b, I. A. Zgolich^a,
T. A. Shalygina^a, and G. D. Sadritdinova^a

^aTomsk State University of Architecture and Building, Tomsk, 634003 Russia

^bNational Research Tomsk Polytechnic University, Tomsk, 634050 Russia

*e-mail: riklaz@mail.ru

Received October 11, 2017

Abstract—The effect of the deformation axis orientation on the length and the strength of dislocation junctions in fcc single crystals has been studied within the model of interdislocation contact interactions, which includes the formation of a dislocation reaction and a change in a dislocation configuration under stress in three-dimensional space. The probabilities of failure of a dislocation junction under stress, the formation of indestructible dislocation junctions, and the formation of long strength dislocation barriers capable of limiting the shear zone have been determined.

Keywords: reacting dislocations, glide dislocations, forest dislocations, dislocation junctions, breaking stress of dislocation junctions, long strength barriers

DOI: 10.1134/S0036029518100117

INTRODUCTION

The study and the description of the physical picture of the plasticity and the strength of crystals need a consideration of the interaction of glide dislocations with a dislocation structure, giving a preference to the contact interactions of dislocation of noncoplanar slip systems, since they provide main elementary plasticity acts. The dislocation junctions that form upon the interactions of reacting dislocations belong to the most “strength” static stoppers, which are capable of retarding glide dislocation motion.

The dislocation motion resistance due to overcoming reacting forest dislocations was estimated for the first time in the framework of the simplest Schoek–Fridman model [1], which contains a number of simplifying assumptions because of the complexity of the problem. Then, the interactions of reacting dislocations were studied in a number of works (for example, [2–4]) using this model, in which some simplifications were weakened. As a result, some disadvantages and limitations were revealed in the solution to the problem, and they could not be overcome in the framework of this simplest model.

The new model of interdislocation contact interactions [5] enables one to overcome a number of limitations of the simplest model and to solve a number of problems, including the determination of junction failure conditions and the formation of long strength barriers for different deformation axes at an arbitrary

intersection of reacting dislocation segments, i.e., in a real three-dimensional setting. The substantial influence of dislocation junctions and annihilation zones on glide dislocations was confirmed by imitation simulation [6, 7], 3D simulation of dislocation dynamics [8–13], experimentally [14], and in the case of in situ deformation [15]. The aim of this work is to determine the strength and the probability of failure of the dislocation junctions in fcc crystals at various deformation axis orientations.

SIMULATION OF A DISLOCATION CONFIGURATION UNDER STRESS

Each deformation axis is characterized by the Schmid factor in primary and secondary slip systems and a set of dislocation reactions. Five reactions occur for the [100] deformation axis and only two reactions for the [101] orientation (Table 1).

For example, we consider the reaction $BA, d + AD, c = BD, c$ (Fig. 1). Reacting dislocation PQ slipping in plan (d) intersects with reacting forest dislocation MN (plane (c)) and forms dislocation junction EF disposed at the line of intersection of the planes of reacting dislocations (Fig. 1). The dislocation configuration is changed, triple dislocation nodes E and F are shifted along the junction line, occupying new positions K and L , and the junction length becomes equal to KL under stress τ . The introduction of coordinate system

Table 1. Dislocation reactions in fcc single crystals as functions of the deformation axis orientation

Deformation axis	Reaction number	Type of reaction	Equation of reaction
[101]	1	3a	$BA, d + DB, a = DA$
	2	4a	$BA, d + DC, a = BD/AC$
$[\bar{1}11]$	1	1a	$BA, d + DB, c = DA, c$
	2	2a	$BA, d + CB, a = CA, d$
	3	3a	$BA, d + DB, a = DA$
[100]	1	1b	$BA, d + AD, c = BD, c$
	2	2b	$BA, d + AC, b = BC, d$
	3	3b	$BA, d + AD, b = BD$
	4	4a	$BA, d + DC, a = BD/AC$
	5	4b	$BA, d + CD, b = BC/AD$

xyz makes it possible to trace the dislocation junction length under stress.

The energy of the formed dislocation configuration is described by function $F(y_1, y_2)$ [5],

$$F(y_1, y_2) = E_1(y_1)d_1(y_1) + E_2(y_1)d_2(y_1) + E_3(y_1)d_3(y_1) + E_4(y_2)d_4(y_2) + E_5(y_2)d_5(y_2) + E_6(y_2)d_6(y_2) - \tau b(S_1(y_1) + S_2(y_1) + S_3(y_2) + S_4(y_2)).$$

Here, y_1 and y_2 are the coordinates of dislocation nodes E and F , respectively; $d_i(y_1), E_i(y_1)$ ($i = 1, 2, 3$)

are the lengths and energies per the unit length of dislocation segments $QE, OE,$ and $NE,$ respectively; $d_i(y_2), E_i(y_2),$ ($i = 4, 5, 6$) are the lengths and energies per the unit length of dislocation segments $PF, OF,$ and $MF,$ respectively (Fig. 1); the latter term is the work done by applied stress τ ; S_i ($i = 1, 2, 3, 4$) is the area swept over by the corresponding segment ($QE, NE, MF,$ and PF) under stress τ ; and b is the modulus of the Burgers vector of the glide dislocation.

Triple dislocation nodes $E(0, y_1, 0)$ and $F(0, y_2, 0)$ have current coordinates. The equilibrium position of triple dislocation nodes E and F will correspond to the

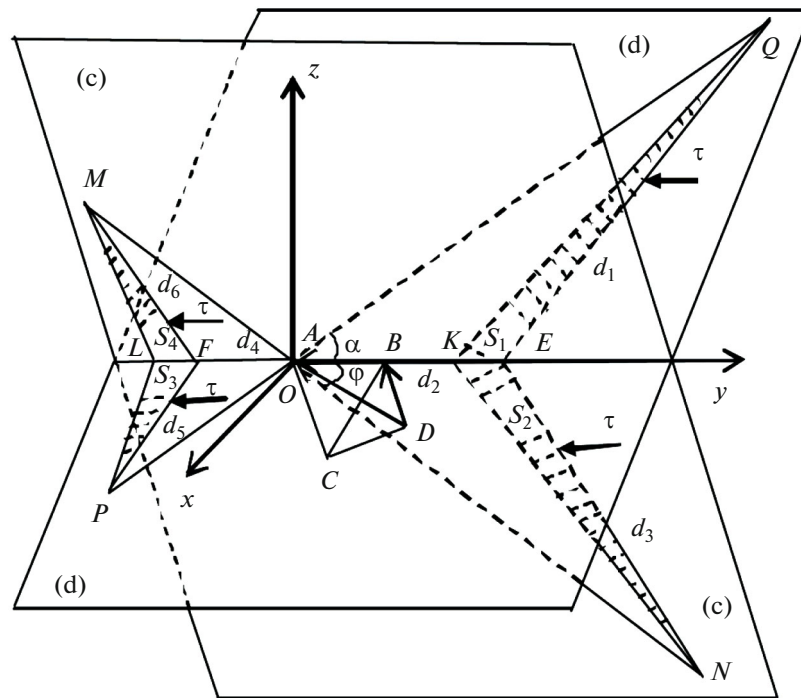


Fig. 1. Geometry of a dislocation junction with initial length EF formed by reacting dislocations: glide dislocation QP and forest dislocation NM ; KL is the junction length under stress τ ; d_i ($i = 1, 2, \dots, 6$) are the lengths of dislocation segments after formation of the junction; S_i is the area swept by corresponding segment ($QE, NE, MF,$ and PF); $ABCD$ is the Thompson tetrahedron; α and ϕ are the initial slope angles of the glide dislocation and the forest dislocation to the junction line, respectively.

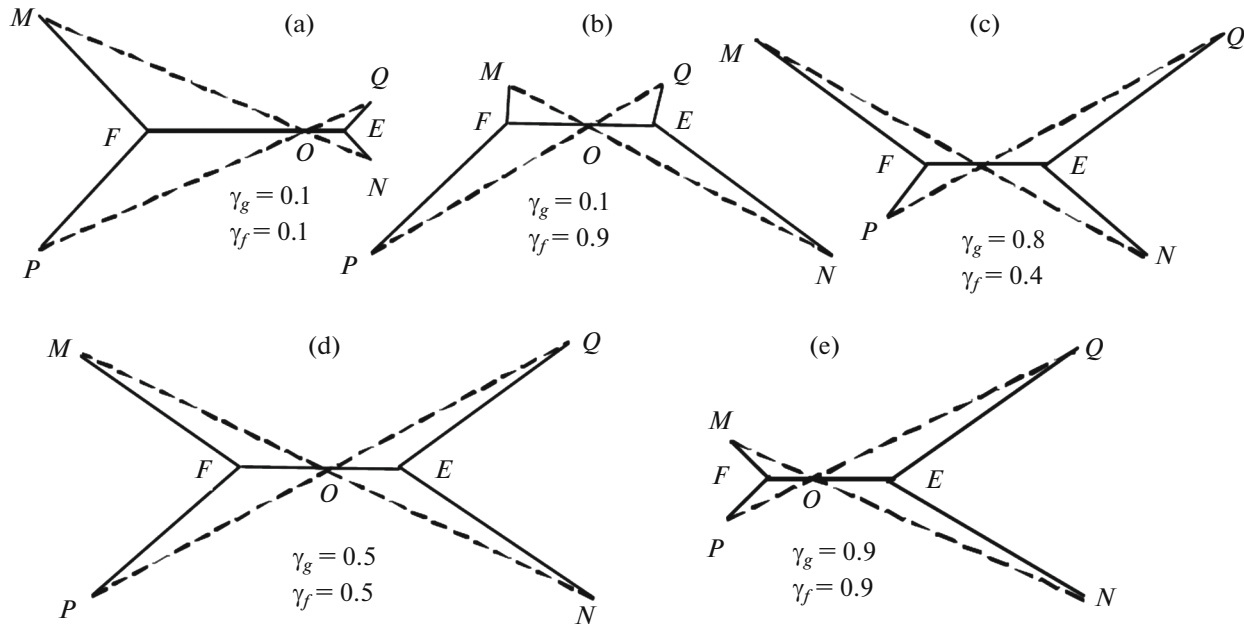


Fig. 2. Schemes of arbitrary intersections of reacting dislocations.

energy minimum of the entire dislocation configuration at the condition that the work of external forces is zero (at $\tau = 0$). The length of dislocation junction EF formed under the given conditions is taken to be the initial length. The position of dislocation nodes K and L is determined from the equilibrium state of the dislocation configuration at a given value of applied stress τ . Assuming that $y_K = y_1$ and $y_L = y_2$, we obtain the coordinates of triple dislocation nodes $K(0, y_K, 0)$ and $L(0, y_L, 0)$. The determination of the energy minimum of a dislocation configuration is analytically reduced to the determination of the minimum of function $F(y_1, y_2)$.

We consider the interactions of reacting dislocations as a function of the ratio of the lengths of the glide dislocation segments $\gamma_g = QO : QP$ and the ratio of the lengths of the forest dislocation segments $\gamma_f = NO : NM$ (O is the point of dislocation intersection). The segments of the reacting glide dislocation PQ and forest dislocation MN are arbitrary separated into parts so that the values of parameters γ_g and γ_f were varied from 0.1 to 0.9. We considered all nine ratios of the lengths of the forest dislocation segments $\gamma_f = NO : NM$ for each ratio of the lengths of the glide dislocation segments $\gamma_g = QO : QP$. A specific scheme of arbitrary intersections of dislocation segments is characterized by a set of parameters γ_g and γ_f . Figure 2 shows the schemes of intersections of dislocation segments for some parameters γ_g and γ_f .

The junction length is changed from the initial value (at $\tau = 0$) to a new length under applied stress τ .¹ One of the “right” reacting segments (QK or NK , Fig. 1) can reach a critical length and lose its stability at some stress τ . In this case, a reacting glide dislocation can pass by the junction. The junction remains unfailed and is not an obstacle to further motion of the glide dislocation; in this case, the junction length is one–two orders of magnitude smaller than the initial length.

In the case when “left” segments PL and ML (Fig. 1) lose their stability, the junction length increases under stress, becomes larger than the initial length, and the junction remains undistorted in the shear zone. Long and strong junctions are observed among these junctions. The junctions whose length under stress is $0.9QP$ (QP is the length of the free glide dislocation segment) are shown separately.

The dislocation configuration under stress was simulated on the basis of the Mathematica system. Applied stresses τ at which the junction was failed due to the coalescence of dislocation nodes or one of reacting segments lost its stability was taken to be rupture stress τ_r of a dislocation junction. The junction strength was determined by rupture stress τ_r . For each dislocation reaction, slopes α of a glide dislocation to the intersection line of reacting dislocations was con-

¹ The mechanisms of changing the junction length under stress were studied in detail earlier [5, 16, 17]. The mechanism of coalescence of dislocation nodes K and L that leads to full failure of a junction has been revealed, and the junctions that remain unfailed under applied stress were also observed.

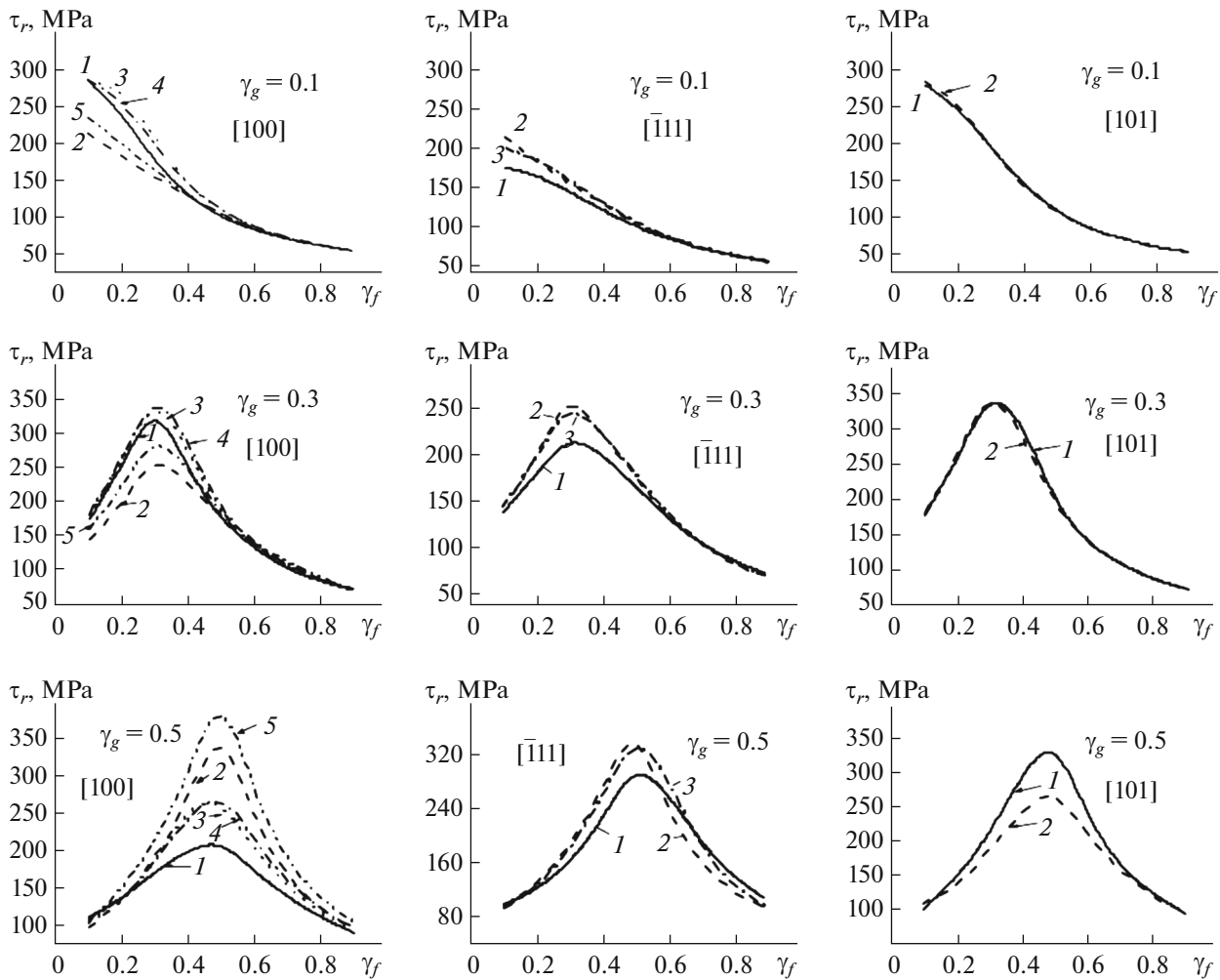


Fig. 3. Rupture stress τ_r vs. the parameter of forest dislocation intersections γ_f (curve numbers correspond to the reaction numbers in Table 1).

sidered from 0° to 90° . In this case, a reaction occurs for all the spectrum of slopes φ of a forest dislocation to the junction line for each angle α (Fig. 1). The calculations were carried out for a dislocation density $\rho = 10^{13} \text{ m}^{-2}$, a shear modulus $G = 5.46 \times 10^4 \text{ MPa}$, the modulus of the Burgers vector $b = 2.5 \times 10^{-10} \text{ m}$, and various intersections of glide dislocation segments (parameter γ_g) with reacting forest dislocations (parameter γ_f).

Based on the results of numerical simulation, we determined the following probabilities: failure of the junction by the mechanism of coalescing dislocation nodes (parameter β_m); the formation of indestructible junctions with the lengths that are smaller than the initial length (parameter β_b), larger than the initial length (parameter β_{rs}), or comparable with the free segment length (parameter β_D). These probabilities were found for each of the deformation axes for the whole spectrum of parameters α , φ , γ_g , and γ_f using the total prob-

ability formula, for which the dislocation reactions are hypothesis.

RESULTS AND DISCUSSION

Figures 3 and 4 show the data on the influence of the orientation of the crystal deformation axis on the junction strength. Rupture stresses τ_r were calculated for glide dislocation slopes $\alpha = 10^\circ$ and forest dislocation slopes $\varphi = 10^\circ$. The junction strength were calculated for each parameter γ_g characterizing the intersection of the glide dislocation segment at the total set of the intersections of forest dislocation segments. According to the obtained results, the most strong junctions form during the intersection of the reacting dislocation segments symmetrical with the respect to the junction line; i.e., when the values of γ_g and γ_f coincide, for example, $\gamma_g = 0.3$ and $\gamma_f = 0.3$ (Fig. 3) or $\gamma_g = 0.7$ and $\gamma_f = 0.7$ (Fig. 4). This situation is observed

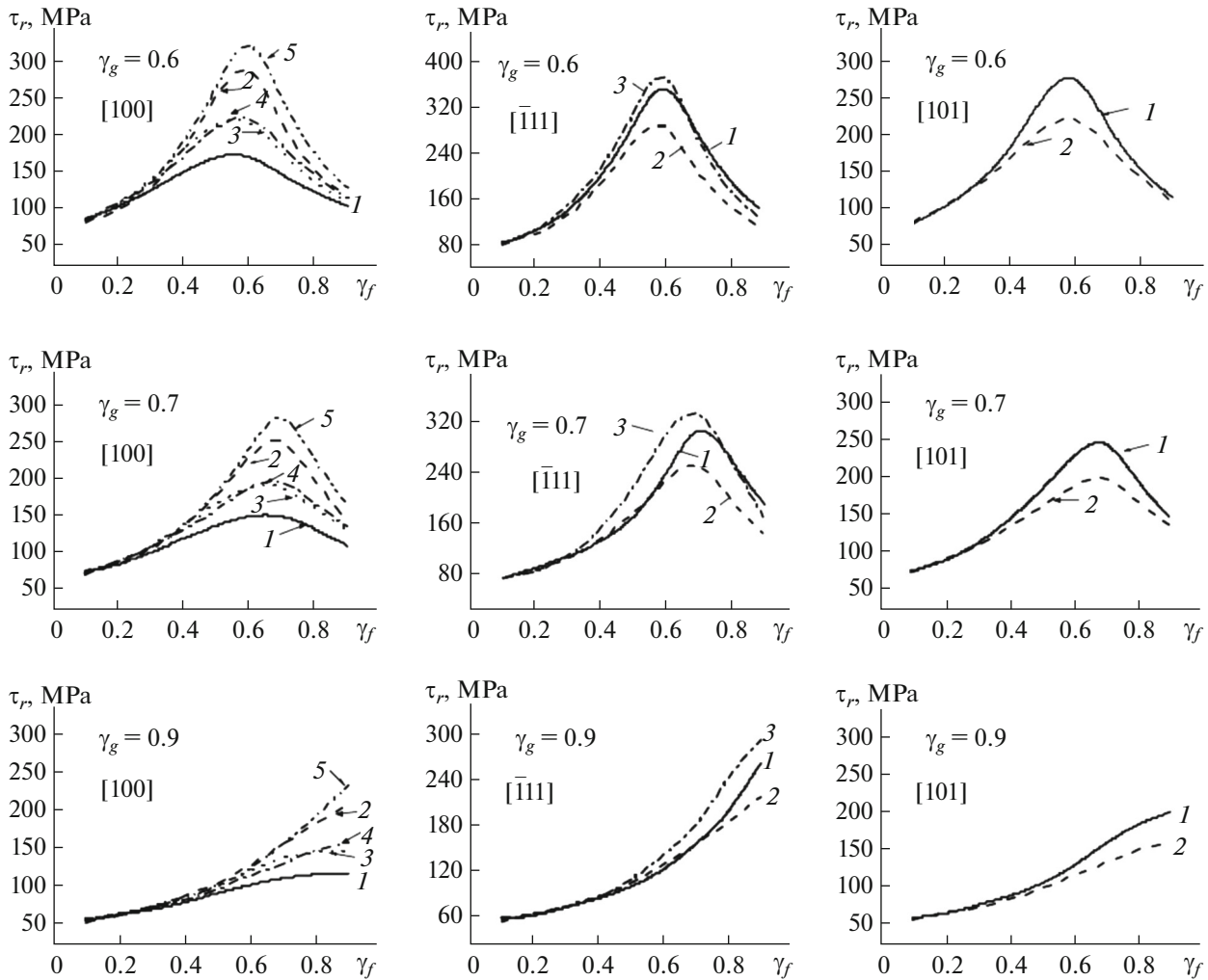


Fig. 4. Rupture stress τ_r vs. the parameter of forest dislocation intersections γ_f (curve numbers correspond to the reaction numbers in Table 1).

for all the orientations of the deformation axis. Conversely, the more asymmetric the reacting dislocation intersection, the less strength the junctions; for example, at $\gamma_g = 0.5$ and $\gamma_f = 0.9$ (Fig. 3) or $\gamma_g = 0.9$ and $\gamma_f = 0.1$ (Fig. 4).

The mean junction strengths were determined from the mean values of the rupture stresses over the entire spectrum of forest dislocations, from $\varphi = 2^\circ$ to the stability angle $\hat{\varphi}$ (the largest angle from the φ angles at which a junction still forms). To find the mean junction strength over all considered orientations of the deformation axis, we used linear average of the rupture stresses over the spectrum of forest dislocations. It was found that the mean strength of the junctions at a fixed intersection of the reacting dislocation segments is dependent on slope α of the glide dislocation. For example, in the case of $\gamma_g = 0.6$ and the [100] and $[\bar{1}11]$ orientations of the deformation axis, the most strong junctions ($\tau_r \approx 200$ MPa) form at $\alpha = 0^\circ$ and the least

strength ($\tau_r \approx 10$ MPa) form at deformation axis [100] and $\alpha = 90^\circ$ (Fig. 5). For deformation axis [101], the most strong junctions ($\tau_r \approx 160$ MPa) form at $\alpha = 0^\circ$, and the least strong ones ($\tau_r \approx 55$ MPa) form at $\alpha = 60^\circ$ (Fig. 6). It should be noted that a dislocation junction does not form in the case of deformation axis [101] and $\alpha = 90^\circ$, since both dislocation reactions do not take place at such slope angles.

It was revealed, as a result of studying the dislocation junction strength at various deformation axis orientations, that 9–21% junctions are completely failed under the applied stress by node coalescence (parameter β_m) (Table 2).

37–47% of the junctions with the length smaller than the initial length remain unfailed in the shear zone (parameter β_{lb}), which increases the density of dislocation fragments and provides accumulation of dislocations. About 35–48% of the long strength junc-

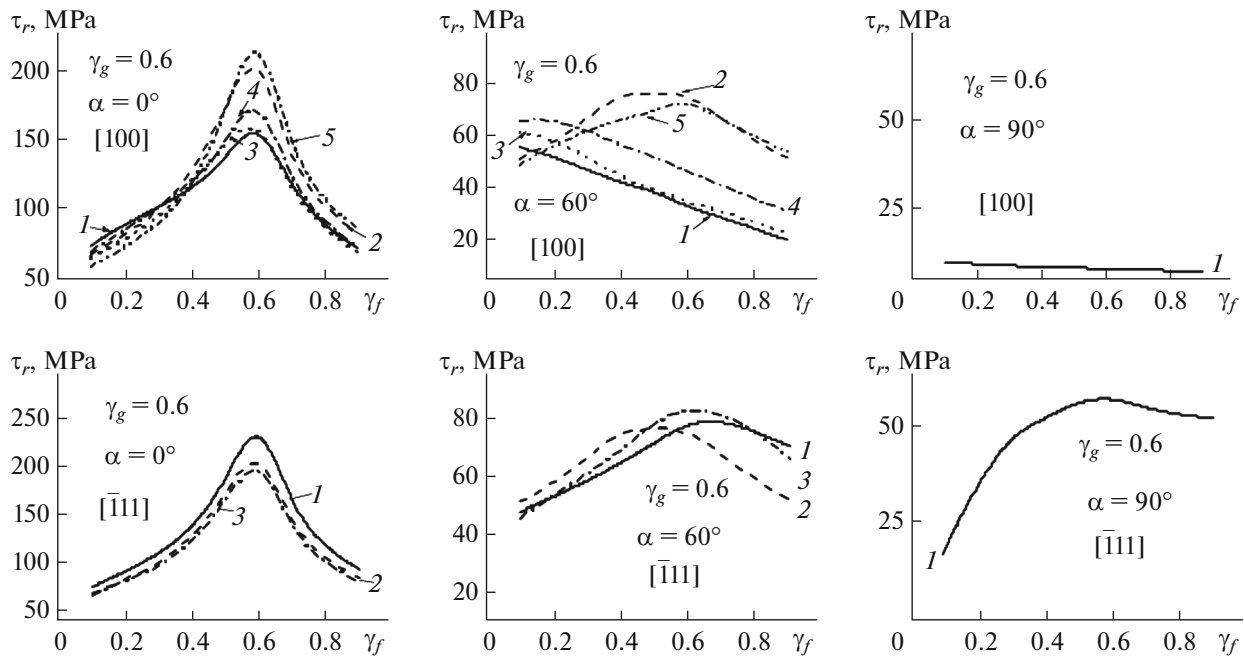


Fig. 5. Mean rupture stresses for deformation axes [100] and $\bar{[111]}$ (curve numbers correspond to the reaction numbers in Table 1).

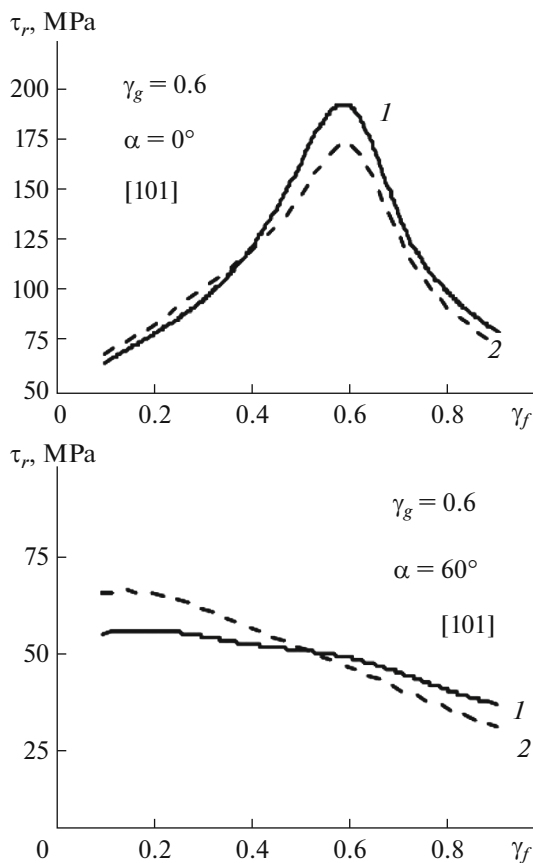


Fig. 6. Mean rupture stresses for deformation axis [101] (curve numbers correspond to the reaction numbers in Table 1).

tions with the lengths larger than the initial length (parameter β_{rs}) also remain unfailed (they are too strength for the acting stress). Only 0.4–0.7% of the long junctions (parameter β_D) can become barriers that restrict the shear zone. Such long strong barriers provide an increase in the dislocation density in the shear zone, determining the contribution to the strain hardening, which was experimentally confirmed [18].

CONCLUSIONS

(1) The failure of a dislocation junction in fcc single crystals under external action by dislocation node coalescence is characteristic in the case of the [101] deformation axis. These junctions provide dislocation slip in the shear zone.

(2) The formation of indestructible junctions, the lengths of which are smaller than the initial length, is characteristic of deformation axis [100]. The formation of long indestructible junctions with lengths larger than the initial length is characteristic of deformation axis $\bar{[111]}$. Such junctions stay in the shear zone, preventing the dislocation motion and contributing to the density of dislocation fragments in the shear zone.

(3) The formation of long strength junctions, whose length can reach 0.9 of the free dislocation segment length, is characteristic of deformation axis $\bar{[111]}$. The formation of such junctions provides the accumulation of dislocations in the shear zone.

Table 2. Probability of dislocation junction failure

Deformation axis	β_m	β_{lb}	β_{rs}	β_D
[101]	0.21	0.37	0.413	0.007
$[\bar{1}11]$	0.091	0.42	0.485	0.004
[100]	0.17	0.47	0.353	0.007

(4) The formation of the long strength junctions that can become barriers restricting the shear zone is most probable for deformation axes [100] and [101].

REFERENCES

- J. Schoek and R. Fridman, "The contribution of the dislocation forest to the flow stress," *Phys. Status Solidi B* **53**, 661–674 (1972).
- K. I. Zlodeeva, N. A. En'shina, and L. E. Popov, "Effect of the character of a stressed state of fcc metal single crystals on the dislocation slip resistance provided by attracting dislocations of secondary systems," *Izv. Vyssh. Uchebn. Zaved., Fiz.*, No. 11, 48–54 (1978).
- W. Puschl, R. Frydman, and J. Schoek, "The strength of the dislocation forest 30° and 60° dislocations," *Phys. Status Solidi A* **74** (1), 211–216 (1982).
- J. P. Michel and G. Champier, "The contribution of pyramidal forest dislocations to the hardening of zinc single crystals," *Phil. Mag. A* **43** (5), 1139–1155 (1981).
- V. A. Starenchenko, M. V. Zgodich, and R. I. Kurinnaya, "Formation of prolonged junctions and barriers as a result of interdislocation reactions in fcc crystals," *Izv. Vyssh. Uchebn. Zaved., Fiz.*, **47** (3), 25–30 (2009).
- A. I. Landau, "The effect of dislocation inertia thermally activated low temperature plasticity of materials. II. Methods of calculations and rate dependences," *Phys. Status Solidi A* **65** (1), 119–125 (1981).
- M. I. Slobodskoi and L. E. Popov, *Study of Slip Phenomenon in Crystals by Imitation Simulation* (TGASU, Tomsk, 2004).
- L. Kubin, B. Devincre, and T. Hoc, "Modeling dislocation storage rates and mean free paths in face-centered cubic crystals," *Acta Mater.* **56** (20), 6040–6049 (2008).
- S. Queyreau, G. Monnet, and B. Devincre, "Slip systems interactions in alpha-iron determined by dislocation dynamics simulations," *Int. J. Plast.* **25** (2), 361–377 (2009).
- S. S. Quek, Z. Wu, Y. W. Zhang, and D. J. Srolovitz, "Polycrystal deformation in a discrete dislocation dynamics framework," *Acta Mater.* **75**, 92–105 (2014).
- Y. Gu, Y. Xiang, S. S. Quek, and D. J. Srolovitz, "Three-dimensional formulation of dislocation climb," *J. Mechan. Phys. Solids* **83**, 319–337 (2015).
- B. Devincre and R. Gatti, "Physically justified models for crystal plasticity developed with dislocation dynamics simulations," *J. Aerospace Lab.*, No. 9, 1–7 (2015). doi 10.12762/2015.AL09–02
- A. D. Rollett, G. S. Rohrer, and R. M. Suter, "Understanding materials microstructure and behavior at the mesoscale," *Mater. Res. Soc. Bull.* **40**, 951–958 (2015).
- R. J. McCabe, A. Mistra, and T. E. Mitchell, "Transmission electron microscopy study of the interaction between a glide dislocation and a dislocation node," *Phil. Mag.* **83** (36), 4123–4129 (2003).
- V. V. Bulatov, L. L. Hsiung, M. Tang, A. Arsenlis, M. C. Bartelt, W. Cai, J. N. Florando, M. Hiratani, M. Rhee, G. Hommes, T. G. Pierce, and T. Diaz de la Rubia, "Dislocation multi-junctions and strain hardening," *Nature* **440**, 1174–1178 (2006).
- M. V. Zgolich, R. I. Kurinnaya, and V. A. Starenchenko, "Rupture of dislocation junctions in fcc materials at the deformation axis orientation [101]," *Vestn. Tambov Univ., Ser. Fiz.* **21** (3), 997–998 (2016).
- R. I. Kurinnaya, M. V. Zgolich, and V. A. Starenchenko, "Strength of dislocation compounds in fcc single crystals with deformation axis $[\bar{1}11]$," *Izv. Vyssh. Uchebn. Zaved., Fiz.* **60** (3), 144–149 (2017).
- L. A. Teplyakova, T. S. Kunitsina, N. A. Koneva, and E. V. Kozlov, "Regularities of the formation of a netlike dislocation structure in the Ni₃Fe alloy single crystals," *Izv. Ross. Akad. Nauk, Ser. Fiz.* **68** (10), 1456–1461 (2004).

Translated by Yu. Ryzhkov